Environmental Science and Pollution Research
https://doi.org/10.1007/s11356-018-2478-0

APPROPRIATE TECHNOLOGIES TO COMBAT WATER POLLUTION

Role of organic fouling layer on the rejection of trace organic solutes by nanofiltration: mechanisms and implications

Zhendong Gan[1] · Xing Du[2] · Xuewu Zhu[1] · Xiaoxiang Cheng[3] · Guibai Li[1] · Heng Liang[1]

Received: 25 March 2018 / Accepted: 1 June 2018

Abstract

To investigate how the organic fouling layers on nanofiltration (NF) membrane surface and the strong matrix effect (particularly by Ca^{2+}) influence the rejection of trace organic compounds (TOrCs), filtration experiments with two TOrCs, bisphenol A (BPA) and sulfamethazine (SMT), were carried out with virgin and organic-fouled NF membrane. Organic fouling layer on the membrane was induced by sodium alginate (SA) at different concentrations of Ca^{2+}. The results indicated that NF membrane maintained consistently rejection of TOrCs with little influence by membrane fouling at lower Ca^{2+} concentration. In contrast, organic fouling caused at higher concentration of Ca^{2+} observably restrained the rejections of both BPA and SMT. Furthermore, based on the cake-enhanced concentration polarization (CECP) model, the rejection of TOrCs was divided to the real rejection and the mass transfer coefficient. Moreover, it was found that the decrease in rejection resulted by organic fouling was due to the real rejection that was restrained by fouling layer with irregular impact on the mass transfer coefficient. Although the mechanism of trace compounds rejection was complex, the controlling factors varied among foulants. Nevertheless, the steric effect of the cake layer played an important role in determining solute rejection by organic-fouled NF membrane.

Keywords Nanofiltration membrane · Organic fouling · Trace organics · Cake-enhanced concentration polarization model

Introduction

Nanofiltration (NF) membranes are increasingly being used in water treatment due to the increasing demand for high-purity drinking water from contaminated sources especially the occurrence of a large number of trace organic compounds (TOrCs) in water sources (Drewes et al. 2003; Kolpin et al. 2002). NF is an effective membrane technology for the retention of TOrCs as the majority of the TOrCs have a molecular weight within 150–500 Da that is efficiently covered by the NF with the molecular weight cut-off about 200–1000 Da (Bellona et al. 2004; Snyder et al. 2003). In addition, according to previous studies on the rejection of trace organics by NF/RO, for some TOrCs with smaller molecular weight, their rejection by the NF is influenced by the following membrane–solute interactions: steric hindrance (sieving effect), Donnan interactions, and non-electrostatic membrane–solute interactions (Bellona et al. 2004; Kiso et al. 2001; Plakas and

Responsible editor: Bingcai Pan

✉ Heng Liang
hitliangheng@163.com

Zhendong Gan
ganzhendong_hit@163.com

Xing Du
hitduxing@163.com

Xuewu Zhu
zhuxuewu1314@163.com

Xiaoxiang Cheng
cxx19890823@163.com

Guibai Li
hitsteven@gmail.com

[1] State Key Laboratory of Urban Water Resource and Environment (SKLUWRE), Harbin Institute of Technology, Harbin 150090, China

[2] School of Civil and Transportation Engineering, Guangdong University of Technology, Guangzhou 510006, China

[3] School of Municipal and Environmental Engineering, Shandong Jianzhu University, Jinan 250101, China

Published online: 11 June 2018

Karabelas 2012; Schäfer et al. 2003; Shan et al. 2009; Verliefde et al. 2009).

Despite NF is superior to other technologies in the removal of TOrCs, complete removal is still difficult to achieve, especially with the presence of membrane fouling. Membrane fouling, the bottleneck of membrane technology, not merely results in flux decline but also potentially influences TOrCs rejection (Hajibabania et al. 2011; Kiso et al. 2001; Schäfer et al. 2003). The retention behavior of TOrCs by the fouled membrane is complicated and the conclusions are not consistent. Studies that have investigated the effects of membrane fouling on rejection have reported varying observations, with some reporting a decline in rejection of organics due to fouling (Nghiem and Hawkes 2007; Xu et al. 2006), while others are contrary (Schäfer et al. 2002; Verliefde et al. 2009). No clear explanation for these different observations has been provided in the literature. In general, the cake layer caused by membrane fouling could increase or decrease the rejection of charged compounds according to their charge by electrostatic repulsion and affects the rejection of neutral compounds through the cake-enhanced concentration polarization (CECP) phenomenon (Contreras et al. 2009; Ng and Elimelech 2004; Verliefde et al. 2009). The CECP model was proposed by Hoek and Elimelech which have suggested that the back diffusion of salts from the vicinity of membrane surface is hindered by the presence of the cake layer (Hoek and Elimelech 2003). In addition, this model is not only suitable for salt removal but also for removal of organic matter with the presence of cake layer.

The main limitation of other studies is that previous researchers fail to account for the decrease in permeate flux caused by membrane fouling. According to the solution–diffusion model, the flux is directly related to the rejection of solutes. Therefore, changes in flux might interfere with the study of rejection. In addition to this, the study focused more on the effect of the interaction between the surface of the cake layer and organic matter on the rejection, while neglecting the role of the cake layer itself, especially caused by the synergic effect of organic and ionic foulants.

In this study, the removal of two kinds of TOrCs with different characteristics in a lab-scale NF system was investigated by the clean and the fouled membrane. By changing the content of ions in the feed, different levels of membrane fouling were constructed to explore the influence of inorganic salts in the removal of TOrCs. To apply the CECP model, the retention process was divided into two parts to study, mass transfer coefficient and real rejection. By comparing the changes of the two parameters in the process of rejection, the mechanism of cake layer at different calcium concentration affecting the removal of organics was studied. The results were expected to illustrate the role and mechanism of membrane fouling and cake layer in the removal of TOrCs.

Experimental

Model trace organic compound selection

Two kinds of trace organic compounds (TOrCs) that were purchased from Sigma Aldrich were selected as target model foulants in this study, bisphenol A (BPA) and sulfamethazine (SMT). The organics represent different characteristics in charge and hydrophobicity (see Table 1 and Fig. 1). The concentrated solutions (1 g/L) of chemicals were prepared in a 10.0% (vol) ethanol solution and were refrigerated at 4 °C. The solutes were dosed in the feed water at the concentration of 100 μg/L.

TOrCs analysis

The concentration of two TOrCs in the feed and permeate were detected by using an Agilent 1200 series (Agilent, USA) high-performance liquid chromatography (HPLC) equipped with UV detector at 278 nm. A C18 column was used with binary gradient mobile phases in 25 min. The flow rate was 1 mL/min and the injection volume was 50 μL. Phase A and phase B were acetonitrile and water with 0.2% (vol) acetic acid, respectively. The gradient parameters were summarized in Table 2. Two calibration curves had a correlation coefficient of 0.99 or better.

Membrane and membrane characterization

A commercial polyamide thin nanofiltration membrane (NF-270, Dow Filmtec, USA) was used in this study. This membrane is made of a thin polyamide active layer, a thicker polysulfone supporting layer, and a nonwoven layer. According to the Dow manufacturer, the minimum salt rejection of NF-270 is 97.0% based on the following test conditions: salt concentration of 2000 mg/L $MgSO_4$, pressure of 0.48 MPa, temperature of 25 °C, and 15% recovery. The molecular weight cut-off (MWCO) of the membrane is around

Table 1 Trace organic compounds and their physicochemical properties

Compounds	Formula	MW (g/mol)	Charge (pH = 7)	logP
Bisphenol A (BPA)	$C_{15}H_{16}O_2$	228.3	Neutral	3.43
Sulfamethazine (SMT)	$C_{12}H_{14}N_4O_2S$	278.3	–	0.80

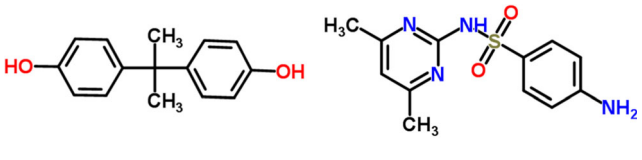

Bisphenol A Sulfamethazine

Fig. 1 Structural formula of BPA and SMT

250 Da, with the mean pore size of 0.84 nm (Mahlangu et al. 2016). The pure water permeability of NF-270 is about 9.6 L/m^2 h bar. The membrane was stored in a 1.0% (wt) $NaHSO_3$ solution at room temperature. Before filtration, the new membranes were soaked in Milli-Q water for approximately 24 h.

Nanofiltration set-up and protocol

Filtration experiments were carried out with a commercial cross-flow flat sheet membrane cell (CF042D, Sterlitech, USA) with the effective membrane area of 42 cm^2. The feed water was pumped into the cell by a high pressure pump (WT3000, Longer, China) from a 2 L glass feed bottle. A thermostatic bath was equipped to maintain a constant feed water temperature (25 ± 2 °C) in order to avoid the disturbances of rejection and flux caused by temperature. There were two stainless steel valves on the polythene tubing, concentrate control valve and bypass control valve. The transmembrane pressure (TMP) was fixed at 0.5 MPa, and the cross-flow flux was adjusted from 5 to 25 L/h by adjusting the two valves. During the filtration experiment, all of the permeate water and concentrate water were returned to the feed bottle to keep the concentration constant. And at least two parallel filtration set-ups were used as replicates.

Before the experiments, the membrane was compacted with Milli-Q water at 0.5 MPa for 12 h with the cross-flow flux of 25 L/h. After compaction, filtration experiments were divided into four steps. The first step was equilibration between the ionic solution and membrane surface. A total of 1.5 mM calcium was added into the feed water as $CaCl_2$ (Aladdin, China), and the concentration of NaCl (Xilong, China) was 15.5 mM in order to maintain the total ionic strength at 20 mM. The filtration was followed with the salt solution for 2 h with the same operating conditions of compaction. Then, the valves were adjusted so that the initial flux was 48 L/m^2 h, which was determined by electronic scales. Secondly, after equilibration, two TOrCs were added to the feed at 100 μg/L to investigate the rejection of solutes by the clean membrane. The applied flux was 48 L/m^2 h, and the cross-flow flux was first set at 5 L/h. Due to adsorption of the solutes by membrane surface (Wang et al. 2015a, b), after the filtration was carried out 24 h, the feed and permeate water were sampled for analysis; meanwhile, the filtration flux was determined to maintain a constant flux. Then, the cross-flow flux was set at 10, 15, 20, and 25 L/h, and the filtration tests followed the same procedure with 5 L/h. The third step was membrane fouling. Sodium alginate (SA) (Sigma Aldrich, Belgium) was selected as model foulant. To speed up membrane fouling and cake layer formation, high foulant concentration was used, in which 20 mg/L SA was added in the feed water after step 2 at flux of 48 L/m^2 h and cross-flow flux of 25 L/h. The filtration flux was determined every 3 h. The membrane was expected to be completely covered by cake layer as the flux was down to half of the initial flux (about 24 L/m^2 h). Then, the feed water was drained off, and the membrane was flushed with Mill-Q water for 10 min. The last step was quantifying the rejection of TOrCs by the fouled membrane. The filtration process was with the same operation procedure of step 2 except for pressure that was adjusted to a constant flux with step 2. After 24 h, the feed and permeate water were collected for concentration analysis. In general, the flux was constant at 48 L/m^2 h except for the membrane fouling process.

In order to investigate the effects of divalent cations, the experiments were carried out with different concentrations of calcium. The concentration of calcium was set at 0 to 6 mM, and the concentration of NaCl was adjusted accordingly to maintain the total ionic strength at 20 mM. In each ionic condition, the filtration experiments followed the same procedure mentioned previously. Solution pH was controlled at 7.0 ± 0.2 by diluting HCl and NaOH. Table 3 provides a summary of the steps carried out with filtration tests.

Table 2 Gradient parameters for HPLC analysis of TOrCs

Run time (min)	Phase B:Phase A
0	30:70
5	50:50
12.5	75:25
17.5	50:50
25	30:70

Cake-enhanced concentration polarization model

For membrane filtration process, concentration polarization (CP) that is caused by the increase of solute concentration on the membrane surface is ubiquitous and one of the primary sources of flux decline. Especially for salt-rejecting membranes, RO and NF, CP aggravates the osmotic pressure difference between the feed and the permeate water. The osmotic pressure is also enhanced in the presence of fouling layer due to a combination of hindered back diffusion of salt ions and organic or colloidal layers, which results in an increased solute concentration on the membrane surface. This accounts for both concentration polarization of ions and hindering of back diffusion of cake layer, which is referred to as cake-enhanced

Table 3 Summary of operation parameters and physicochemical properties of feed for filtration experiment

Steps	Flux (L/m^2 h)	Cross-flow flux (L/h)	TOrCs (μg/L)	SA (mg/L)	$CaCl_2$ (mM)	NaCl (mM)
1	48	25	0	0	0–6	20–2
2	48	5–25	100	0	0–6	20–2
3	TBD	25	100	20	0–6	20–2
4	48	5–25	100	0	0–6	20–2

concentration polarization (CECP) (Hoek and Elimelech 2003). According to the results of CECP, the rejection of TOrCs is determined by solute concentration on the membrane surface instead of the feed concentration (Contreras et al. 2009; Vogel et al. 2010). Therefore, the observed rejection (R_{obs}) relates to the feed solute concentration (C_f) and permeate (C_p); meanwhile, the real rejection (R_r) is determined by the solute concentration on the membrane surface (C_m) and C_p as shown in Eq. (1) and Eq. (2):

$$R_{obs} = 1 - \frac{C_p}{C_f} \tag{1}$$

$$R_r = 1 - \frac{C_p}{C_m} \tag{2}$$

During the filtration process, mass balance analysis is conducted and incorporated into the rejection equations, Eq. (1) and Eq. (2), and solving the equation over the CP laminar boundary layer with thickness δ, as shown in Eq. (3):

$$\ln\frac{1-R_r}{R_r} = \ln\frac{1-R_{obs}}{R_{obs}} - \frac{J_w}{k} \tag{3}$$

where J_w is water flux and k can be determined from empirical correlations, which are a function of the low conditions in a membrane system, the nature of the solution, and the geometry of the system (Cornelissen et al. 2005). According to the previous study (Porter 1972), k could be derived indirectly from a nondimensional function as shown in Eq. (4):

$$Sh = A(Re)^{\alpha}(Sc)^{\beta} \tag{4}$$

where Sh is the Sherwood number that is related to k, D, and the equivalent hydraulic diameter of cross-flow channel (d_h)($Sh = kd_h/D$). Re is the Reynolds number, Sc is the Schmidt number, and α and β are determined by the change of velocity field and concentration field in the channel, and A is a constant. For this experiment that used rectangle cross-flow channel and laminar flow in the channel, generally k is given by the following equation (Porter 1972):

$$k = 0.816\left(\frac{6u}{bL}D^2\right)^{0.33} = 0.816\left(\frac{6Q}{ab^2L}D^2\right)^{0.33} \tag{5}$$

where u is the cross-flow velocity, Q is cross-flow flux, and b and L are the height and length of cross-flow channel, respectively. Proportional constant (c) is defined as shown in Eq. (6), and the equation for k is therefore presented as follows:

$$c = 0.816\left(\frac{6}{ab^2L}D^2\right)^{0.33} \tag{6}$$

$$k = cQ^{0.33} \tag{7}$$

Finally, the equation for the transfer coefficient (Eq. (7)) is incorporated into the rejection equations (Eq. (3)) as shown in Eq. (8):

$$\ln\frac{1-R_{obs}}{R_{obs}} = \ln\frac{1-R_r}{R_r} + \frac{J_w}{c}Q^{-0.33} \tag{8}$$

In this study, the water flux (J_w) and cross-flow flux (Q) are controllable parameters, as observed rejection (R_{obs}) is determined by experiments. In Eq. (8), it is considered as a linear function between $Q^{-0.33}$ and $\ln\frac{1-R_{obs}}{R_{obs}}$, that $\ln\frac{1-R_r}{R_r}$ is the intercept and $\frac{J_w}{c}$ is the slope of the function. Thus, Eq. (8) is then used to calculate the real rejection (R_r) and the mass transfer coefficient (k) that is related to c by a series of experimental data.

Results and discussion

Rejections of TOrCs by clean membrane

The rejections of two TOrCs during the filtration with the virgin membrane were investigated. The filtration flux remained constant at 48 L/m^2 h, and the first sample was collected after 24 h when the filtration had been carried out to stability to reduce the influence of flux and solute adsorption on the membrane surface. The average rejection of SMT was about 68.83%, and in contrast, the rejection of BPA was merely 28.26% (Fig. 2). The rejection from the NF membrane could be attributed to three kinds of interactions: steric hindrance effect, Donna interaction, and non-electronic affinity interaction, like hydrophobic adsorption (Childress and Elimelech 2000; Mohammad et al. 2015). There was Donna interaction between the nanofiltration membrane surface and the SMT molecule, which dissociated the amino group and sulfonamide group in water. Therefore, the electrostatic repulsion of the nanofiltration membrane increased its rejection.

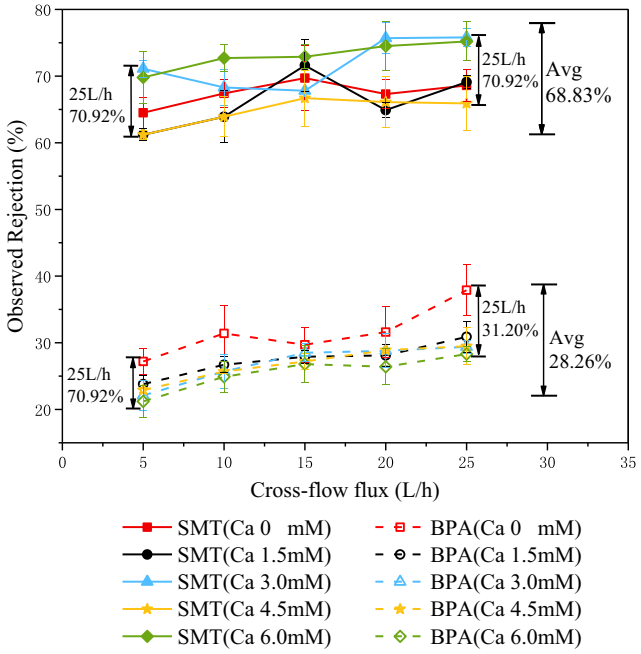

Fig. 2 Observed rejection of SMT and BPA with different cross-flow fluxes at various calcium concentrations (permeate flux = 48 L/m^2 h, cross-flow flux = 5–25 L/h, pH = 7 and total ionic strength = 20 mM)

However, the BPA without any dissociative groups was neutral in the general water environment, so that the removal of BPA only relied on steric hindrance and hydrophobic adsorption. It might be the reason why the rejection of BPA was much lower than the SMT.

According to Fig. 2, the rejections of all TOrCs were slightly increased with cross-flow flux up to 25 L/h. This might be attributed to the decrease of concentration polarization effect caused by the cross-flow. For clean membrane, the solute rejection was restrained by the CP from itself. With the wash effect of cross-flow, the concentration of solutes on the membrane surface decreased. Therefore, the effect of CP was relieved with the increase of cross-flow flux, and the rejection was promoted. The results conformed to the researches about control of CP (Ahmad et al. 2005; McCutcheon and Elimelech 2006).

Effects of cations on fouling behavior

Figure 3a shows the decline in flux as a function of filtration time with the different calcium concentrations. In general, the normalized flux (J/J_0) decreased to 0.57 at the end of filtration about 50 h when filtering was 20 mg/L SA in the absence of calcium. The flux suffered a more severe decline when calcium was added, which was not a simple linear relationship with the concentration of calcium. The flux slightly decreased to 0.55 when the feed contained 1.5 mM Ca^{2+}. Then, more cations caused more serious fouling, in which at the end of filtration, the flux was only about 0.41 at 3 mM.

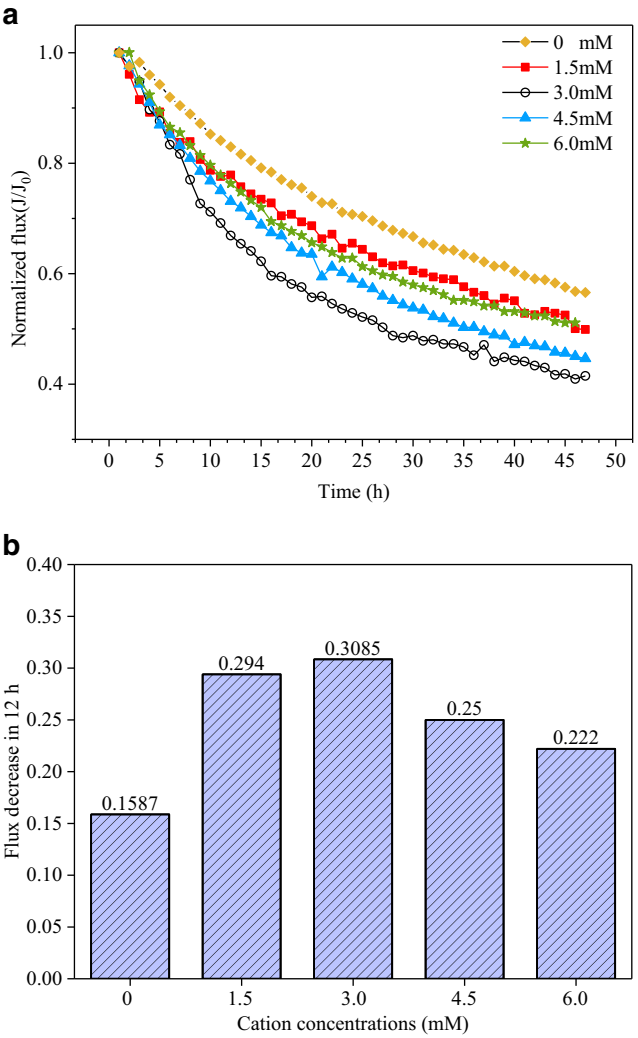

Fig. 3 Normalized flux declines with divalent cation concentrations ranging from 0 to 6 mM: (**a**) during whole experiment (about 48 h); (**b**) the amount of flux decline at the first 12 h

However, compared with 3 mM calcium, if more calcium was added to the feed water, the level of membrane fouling was reduced. The values of flux declined to 0.45 and 0.51, when 4.5 and 6 mM calcium was added to the feed, respectively. Therefore, under the experimental conditions in 20 mg/L SA, the tendency of membrane fouling showed that within limits, a higher cation concentration (3 mM) led to a higher flux decline than that at lower concentration (1.5 mM), while at high concentration (3 mM–6 mM), a lower cation concentration led to a higher flux decline than that at higher concentration.

Besides the values of flux decline, the rate of membrane foiling had the same trend. Figure 3b shows the normalized flux decline in the first 12 h of filtration to express the rate of initial fouling. Similar to Fig. 3a, there was an inflection point at 3 mM, in which the speed of flux decline was the fastest at. The value at 3 mM might be the critical calcium concentration that caused the most severe membrane

fouling. This might be attributed to the sufficient charge screening and the compression of electrostatic interaction forces at a higher cation concentration, and the existence of critical concentration was evidenced by Mo and Al (Aoustin et al. 2001; Mo et al. 2011). At high calcium concentration, the calcium-bridging effect caused the significant formation of SA aggregates and reduced the amount of dissolved organic carbon that might aggravate membrane fouling. However, with the flush effect of cross-flow, the effective rate of SA toward the membrane and the fouling it causes occur more slowly (Mo et al. 2011). These observations are in agreement with previous studies about ultrafiltration and nanofiltration (Costa et al. 2006; Li and Elimelech 2004; Wang et al. 2015a). It should be noted that the experimental results only indicated that 3 mM of calcium caused the most serious membrane fouling under 20 mg of SA, rather than it was the most unfavorable filtration condition.

Effects of cations on retention behavior

The presence of calcium in feed water emitted various effects, like compression of electrostatic interaction forces and calcium bridging, which not only influenced membrane fouling but played the part of TOrCs retention process. For clean membrane, with the change of cation concentration, the rejections of solutes remained relatively stable (Fig. 2). For fouled membrane, according to previous studies (Comerton et al. 2009; Sadmani et al. 2014; Yang et al. 2017; Zhao et al. 2016; Zhao et al. 2013), the presence of calcium and organic matters could influence solutes rejection significantly. In the first part of the experiment, the TOrCs in low concentration (100 μg/L) were rejected by the virgin membrane in pure water with constant ionic strength. Moreover, BPA did not contain any functional groups that can dissociate within the common pH range, as SMT can easily ionize amino and sulfonamide groups. Due to a constant background ionic strength in the solution, the change of calcium had no significant influence on the mechanism of nanofiltration membrane retention, and the effect of calcium, like calcium bridging, was weak without high molecular weight organic matters and hardly influences the filtration process.

In contrast, an obvious increase in permeation of two kinds of trace organics was observed for the fouled membrane with the addition of SA and calcium, especially in higher calcium concentration. The relative change in rejection of TOrCs with different cross-flow fluxes was plotted as a function of calcium concentration (Fig. 4). In general, with the increase of calcium concentration, a gradually increasing trend of the permeation values of solutes was observed. For SMT (Fig. 4a), the permeation of solute was not influenced by fouling cake layer obviously with the absence of calcium. When the

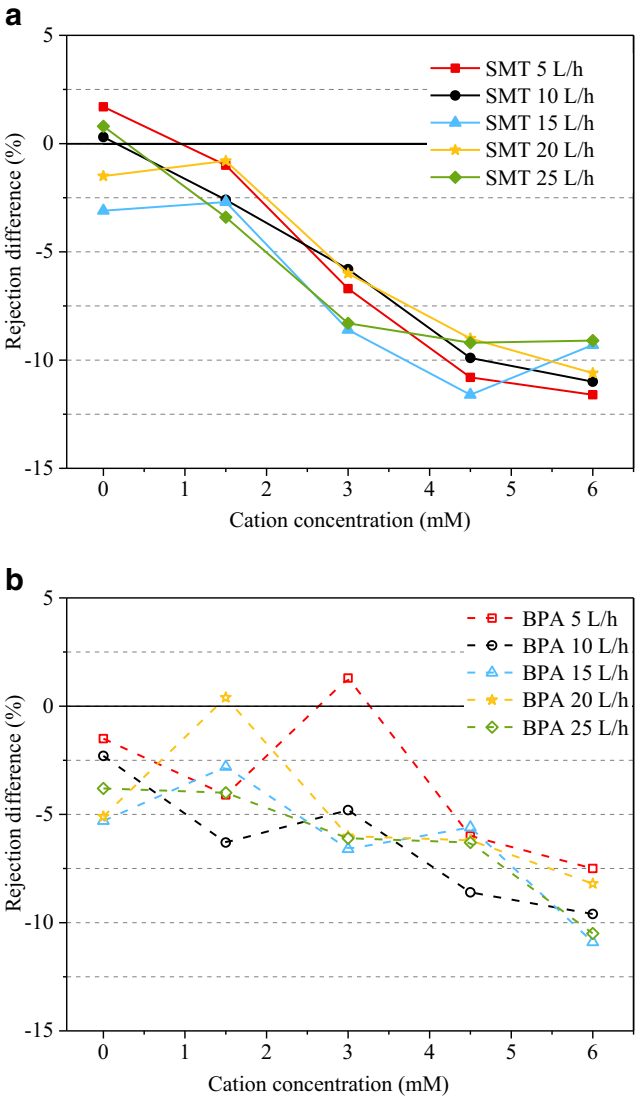

Fig. 4 Relative change of rejection as a result of membrane fouling in the presence and absence of calcium: (**a**) SMT; (**b**) BPA

concentration of calcium was 1.5 mM, the rejection of SMT for the fouled membrane was slightly changed. While the concentration of calcium was increased to 3 mM, cake layer began to have a significant effect on the rejection of solute, resulting in a decrease in rejection rate, about 7.5%. Afterward, increasing the calcium concentration, the effect of membrane fouling on the rejection of SMT was strengthened, and the rejection was reduced more. At the end of the experiment, the concentration of calcium was 6 mM, and the relative change of rejection was more than 10%. BPA had a similar trend of rejection, but the changes were milder (Fig. 4b). During the whole experiment, in the range of 0–6 mM calcium, the cake layer caused by membrane fouling reduced the rejection of BPA, and with the increase of calcium concentration, the rejection decreased more obviously but generally less than SMT. The rejection of BPA was slightly decreased about 2–5% for fouling membrane without the

presence of calcium. With 6 mM calcium added to the feed water, the relative rejection was about 7.5–10%.

As SMT and BPA had different characteristics in electrical and hydrophobic properties (see Table 1), they were affected differently in the retention process. For SMT, a slightly decrease in the permeation of trace organics was observed for fouling in the absence of calcium because of decreases in trace organic concentration at the membrane surface due to electrostatic repulsion (Mahlangu et al. 2016). Furthermore, previous studies have extensively shown that membrane surfaces typically become neutralized when fouling occurs in the presence of calcium according to membrane zeta potential based on the Helmholtz-Smoluchowski equation (Mahlangu et al. 2014; Nyström et al. 1994). Meanwhile considering the difference in the nature of the two and the similarity of the observations, the decrease of rejection for fouling with the addition of calcium can indeed be partially attributed to steric hindrance and non-electrostatic membrane–solute affinity interactions caused by cake layer and concentration polarization (Mahlangu et al. 2016). Moreover, at the same calcium concentration, the relationship between cross-flow flux and rejection of solutes did not appear to be obvious. However, the cross-flow flux is related to fouling process, so the relationship between cross-flow flux and rejection needed further analysis through the CECP model.

Cake-enhanced concentration polarization model analysis

In the last section, the relative change in permeation with different cross-flow fluxes was related to the concentration of calcium to compare the effect of different concentration cations on TOrCs rejected by the fouled membrane. According to the CECP model, previous results were obvious rejection. In order to investigate the mechanism of the effect of cake layer in the retention process, CECP model analysis of observed rejection and cross-flow flux is obtained. Based on Eq. (8), through the determination of the observed rejection of different cross flows under constant flux, $Q^{-0.33}$ and $\ln\frac{1-R_{obs}}{R_{obs}}$ were model-fitted, and a linear relationship can be obtained. Then, the resulting straight line was extrapolated, the intercept obtained was a function of the real rejection, and the slope of the line was a function of proportional constant c that was about the mass transfer coefficient. Figure 5 illustrated the fitting process using 6 mM Ca^{2+} as an example. Tables 4 and 5 were the fitting equation and the correlation coefficient R^2 of the clean membrane and the fouled membrane under various Ca^{2+} concentrations.

As can be seen from Tables 4 and 5, for the clean membrane, the correlation coefficient was relatively high, indicating that the model had a high degree of fitness, while the correlation was relatively low for the fouled membrane. This

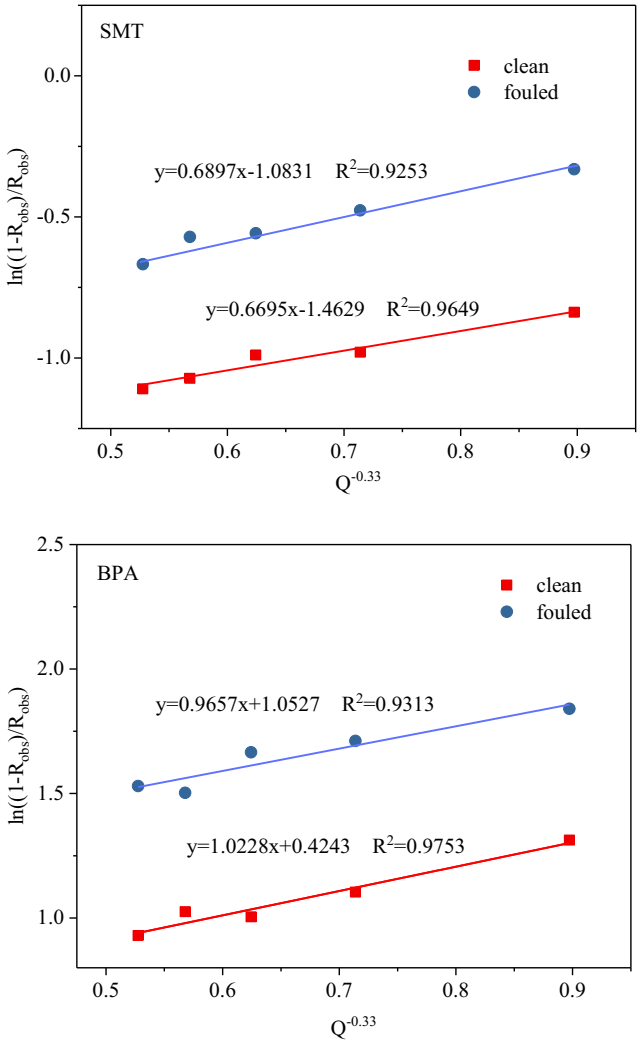

Fig. 5 CECP model fitting curve (at 6 mM calcium as an example): (**a**) SMT; (**b**) BPA

might be due to the surface conditions being more complicated and had more influencing factors caused by membrane fouling. On this point, there were not only the concentration polarization but also the reverse diffusion, adsorption, and steric hindrance that caused an effect on the cake layer on the membrane surface. However, it still had certain reference significance as a clear linear relationship was obtained.

According to Eq. (8), the slope of the obtained function was $\frac{J_w}{c}$, where c was the proportional coefficient. As the permeate flux, J_w was constant (48 L/m^2 h) during the test, and the coefficient c can be calculated through the slope. According to Eq. (7), the mass transfer coefficient corresponding to the cross-flow was calculated when c was obtained. Table 6 was the calculation results of the proportional coefficient c. As cross-flow flux was determined, the analysis results of the proportional coefficient were in direct proportion with mass transfer coefficient. Therefore, the influence of membrane fouling on mass transfer coefficient can be obtained by

Table 4 CECP fitting equation and correlation coefficient (R^2) for SMT at different concentrations of calcium

Calcium concentration	Virgin membrane		Fouled membrane	
	Fitted equation	R^2	Fitted equation	R^2
0	$y = 0.4832x - 0.9951$	0.9315	$y = 0.4952x - 1.0986$	0.8825
1.5	$y = 0.5067x - 0.9343$	0.9390	$y = 0.4789x - 0.8001$	0.9521
3	$y = 0.6594x - 1.5998$	0.9547	$y = 0.6687x - 1.2657$	0.9267
4.5	$y = 0.6457x - 1.0255$	0.9403	$y = 0.7205x - 0.6190$	0.8708
6	$y = 0.6695x - 1.4629$	0.9649	$y = 0.6897x - 1.0831$	0.9253

investigating the change of c. Figure 6a showed the effect of membrane fouling caused by different concentrations of calcium on the mass transfer coefficient. It was observed that membrane fouling had an effect on mass transfer coefficient. However, the tendency of the coefficient to increase or decrease was irregular with the concentration of calcium.

Extrapolating the fitting equation obtained in Tables 4 and 5 to calculate the y-axis intercept of the function, it was $\ln\frac{1-R_r}{R_r}$ which the real rejection of TOrCs can be obtained after calculation through. Table 7 showed the real rejection of solutes with the clean membrane and the fouled membrane under different degrees of membrane fouling. As can be seen from Table 7, the real rejection of SMT was around 70–80%, compared with 30–50% of BPA. Obviously, both had a higher real rejection than observed rejection. This phenomenon was consistent with the assumption of the concentration polarization model, that in the concentration polarization layer, the concentration of solute gradually raised, resulting in the highest concentration point in the system on the membrane surface (Hajibabania et al. 2011; Lee et al. 2006; Lee et al. 2004). Thus, the real rejection that compared with the concentration in permeation and on membrane surface where there was the highest concentration was higher than observed rejection that compared with the solutes in the feed and permeate.

The real rejection after the fouling was subtracted from it of the clean membrane to obtain a relative difference in real rejection (Fig. 6b). Similar to the observed rejection, with the increase of calcium concentration, the impact on the real rejection was also more serious. Moreover, the effect of membrane fouling on the real rejection of BPA was more significant than SMT.

Role of CECP on solute permeation through the fouled membrane

In the CECP model, the mass transfer coefficient and the real rejection were used as physical parameters to characterize the retention process of TOrCs during the filtration (with cake layer if the membrane was fouled). Figure 7a was a sketch of the concentration polarization process after membrane fouling. The influence of the cake layer on the mass transfer coefficient was due to the change in the thickness of the concentration polarization layer and the emergence of cake layer that hindered the transfer of solutes. The effect of the cake layer on the real rejection was due to the change of the solid layer thickness and the number of layers, while the real rejection reflected the change of the membrane surface concentration C_m and the permeate concentration C_p.

According to previous studies (Porter 1972), the mass transfer coefficient calculation was determined by the diffusion coefficient of solutes, the size of the cross-flow channel and membrane pore size. The diffusion coefficient was constant during filtration process according to Wilke-Chang equation (Miyabe and Isogai 2011). According to the hypothesis in this experiment, the fouling caused by SA did not affect the pores in the membrane. Thus, the reasons why the membrane fouling had an effect on the mass transfer in concentration polarization layer were the presence of the cake layer that had a sufficient thickness to compress the cross-flow channel height and increase the number of filter layers. For the former, it can be inferred that within the calcium concentration range (0–6 mM), cake layer produced by membrane fouling at various calcium concentrations was so thin that it was negligible

Table 5 CECP fitting equation and correlation coefficient (R^2) for BPA at different concentrations of calcium

Calcium concentration	Virgin membrane		Fouled membrane	
	Fitted equation	R^2	Fitted equation	R^2
0	$y = 1.0945x - 0.0753$	0.9332	$y = 1.0455x + 0.0400$	0.8910
1.5	$y = 0.9651x + 0.4067$	0.9578	$y = 1.008x + 0.5971$	0.9088
3	$y = 1.0528x + 0.2878$	0.9636	$y = 0.9961x + 0.7082$	0.8648
4.5	$y = 0.9365x + 0.3835$	0.8913	$y = 0.9902x + 0.9946$	0.9002
6	$y = 1.0228x + 0.4243$	0.9735	$y = 0.9657x + 1.0527$	0.9313

Table 6 Calculation results of the proportional coefficient c ($\times 10^{-5}$)

Ca^{2+} (mM)	SMT		BPA	
	Clean	Fouled	Clean	Fouled
0.5	1.86	2.02	0.82	0.86
1.5	1.78	1.88	0.93	0.90
3	1.36	1.34	0.85	0.90
4.5	1.39	1.25	0.96	0.91
6	1.34	1.30	0.88	0.93

Table 7 Calculation results of the real rejection (%)

Ca^{2+} (mM)	SMT		BPA	
	Clean	Fouled	Clean	Fouled
0.5	73.6	75.0	52.1	49.3
1.5	71.3	68.8	42.7	38.1
3	81.7	77.1	42.5	33.6
4.5	73.7	66.0	46.5	33.0
6	80.8	72.2	40.3	27.1

relative to the height of the cross-flow channel. Thus, the change of the mass transfer coefficient was irregular.

In contrast, the real rejection of solutes in nanofiltration membranes was greatly affected by membrane fouling as the change of filter layers. In the clean state of nanofiltration membranes, the retention is referred to the retention of organics inside the membrane. While for the fouled membrane with cake layer, solutes are needed to pass through the contaminated layer before the retention by the nanofiltration membrane. The role of the cake layer on the membrane surface for TOrCs might be seen as similar to that of a nanofiltration membrane, that the mass transfer of organics was affected by steric hindrance, hydrophobic adsorption, and electrostatic interaction (Hajibabania et al. 2011; Yangali-Quintanilla et al. 2009). However, by comparing the differences in the characteristics of the two organics (molecular weight, charge, and logP) and the similar results obtained from this study, the effect of cake layer on the mass transfer in TOrCs was mainly due to steric hindrance. Membrane fouling, in particular, caused by high concentrations of calcium, hindered the reverse diffusion of solutes from the membrane surface to cake layer surface,

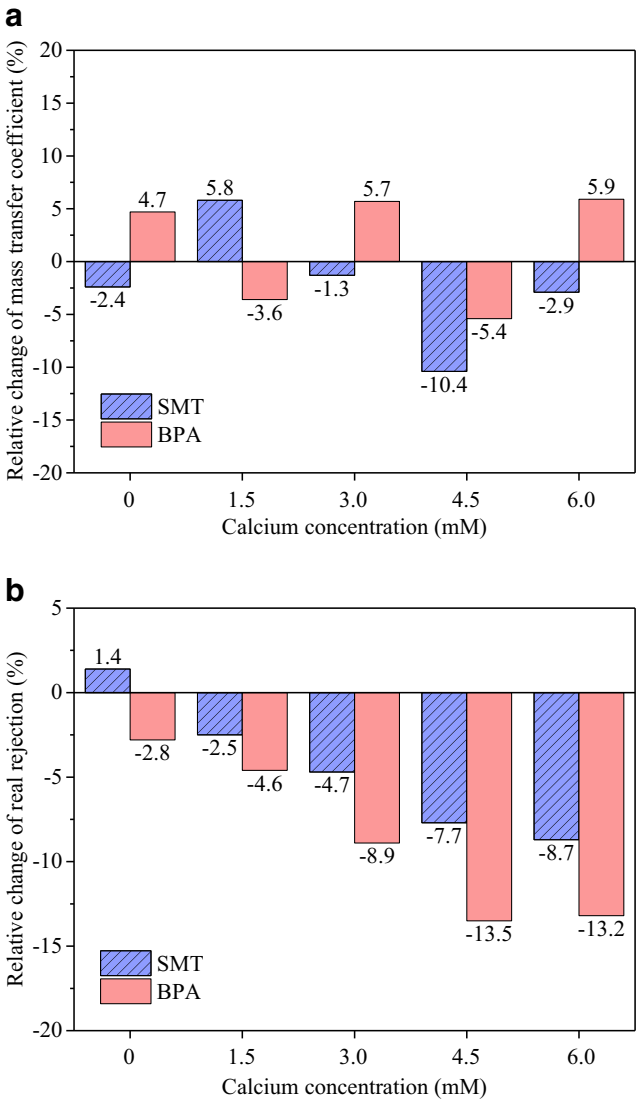

Fig. 6 Relative change of mass transfer coefficient (**a**) and real rejection (**b**) caused by membrane fouling according to CECP model fitting

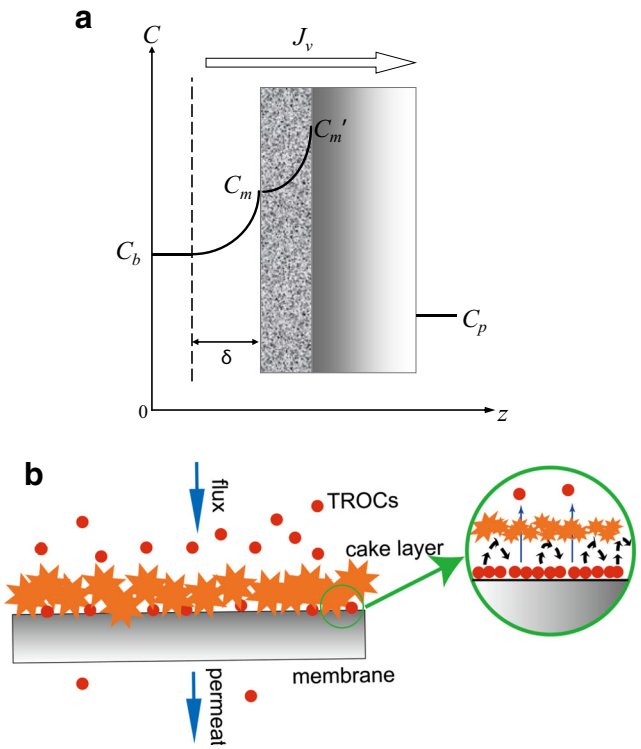

Fig. 7 Diagram of the CECP process: (**a**) the change of concentration; (**b**) the effect of cake layer on hindering the back diffusion

leading to an analogous concentration polarization phenomenon in the cake layer and resulting in an increase of concentration on membrane surface (Fig. 7b). Higher concentration on membrane surface leads to higher values in permeation and therefore lower observed rejection (Fig. 7a).

Conclusions

The TOrCs are rejected efficiently by nanofiltration membrane (NF). However, the rejection of solutes is decreased with membrane fouling especially with the presence of calcium. The rejection of TOrCs by the fouled membrane during the filtration is influenced by several factors. This study aims to investigate the role of cake layer caused by organic fouling on the retention of TOrCs when trace organic rejection for the fouled membranes is compared to that of the virgin membrane. The following observations can be made: (1) the concentration of calcium exists at a critical point (about 3 mM in this study) which causes the most severe membrane fouling and flux decline; (2) the cake layer with relatively low calcium concentration has a weak influence on the removal of organics and is lacking of regularity; and (3) the rejection of solutes is significantly restrained by the existence of cake layer caused by high calcium concentration. Through the cake-enhanced concentration polarization (CECP) model analysis of the results, it is found that the change of the mass transfer coefficient caused by membrane fouling is irregular. However, the effect on the real rejection is similar to the observed rejection, that is it has an inhibitory effect and intensifies with the increase of calcium concentration due to hindering the reverse diffusion of solutes from the membrane surface to cake layer surface by steric hindrance. This work has important implications for further understanding TOrCs in water treatment using membrane processes for drinking water or wastewater reuse. Combining the role of the cake layer and the interface characteristics of the filtration process helps to predict the removal of solutes.

Acknowledgements This research was jointly supported by the National Science Foundation for the Outstanding Youngster Fund (51522804), the National Natural Science Foundation of China (51778170), and the Nanqi Ren Studio, Academy of Environment & Ecology, Harbin Institute of Technology (HSCJ201701).

References

Ahmad A, Lau K, Bakar MA (2005) Impact of different spacer filament geometries on concentration polarization control in narrow membrane channel. J Membr Sci 262:138–152

Aoustin E, Schäfer AI, Fane AG, Waite TD (2001) Ultrafiltration of natural organic matter. Sep Purif Technol 22-23:63–78. https://doi.org/10.1016/S1383-5866(00)00143-X

Bellona C, Drewes JE, Xu P, Amy G (2004) Factors affecting the rejection of organic solutes during NF/RO treatment—a literature review. Water Res 38:2795–2809

Childress AE, Elimelech M (2000) Relating nanofiltration membrane performance to membrane charge (electrokinetic) characteristics. Environ Sci Technol 34:3710–3716

Comerton AM, Andrews RC, Bagley DM (2009) The influence of natural organic matter and cations on the rejection of endocrine disrupting and pharmaceutically active compounds by nanofiltration. Water Res 43:613–622. https://doi.org/10.1016/j.watres.2008.11.003

Contreras AE, Kim A, Li Q (2009) Combined fouling of nanofiltration membranes: mechanisms and effect of organic matter. J Membr Sci 327:87–95. https://doi.org/10.1016/j.memsci.2008.11.030

Cornelissen ER, Verdouw J, Gijsbertsen-Abrahamse AJ, Hofman JA (2005) A nanofiltration retention model for trace contaminants in drinking water sources. Desalination 178:179–192

Costa AR, de Pinho MN, Elimelech M (2006) Mechanisms of colloidal natural organic matter fouling in ultrafiltration. J Membr Sci 281:716–725

Drewes JE, Reinhard M, Fox P (2003) Comparing microfiltration-reverse osmosis and soil-aquifer treatment for indirect potable reuse of water. Water Res 37:3612–3621

Hajibabania S, Verliefde A, McDonald JA, Khan SJ, Le-Clech P (2011) Fate of trace organic compounds during treatment by nanofiltration. J Membr Sci 373:130–139. https://doi.org/10.1016/j.memsci.2011.02.040

Hoek EM, Elimelech M (2003) Cake-enhanced concentration polarization: a new fouling mechanism for salt-rejecting membranes. Environ Sci Technol 37:5581–5588

Kiso Y, Sugiura Y, Kitao T, Nishimura K (2001) Effects of hydrophobicity and molecular size on rejection of aromatic pesticides with nanofiltration membranes. J Membr Sci 192:1–10

Kolpin DW, Furlong ET, Meyer MT, Thurman EM, Zaugg SD, Barber LB, Buxton HT (2002) Pharmaceuticals, hormones, and other organic wastewater contaminants in US streams, 1999–2000: a national reconnaissance. Environ Sci Technol 36:1202–1211

Lee S, Cho J, Elimelech M (2004) Influence of colloidal fouling and feed water recovery on salt rejection of RO and NF membranes. Desalination 160:1–12

Lee S, Ang WS, Elimelech M (2006) Fouling of reverse osmosis membranes by hydrophilic organic matter: implications for water reuse. Desalination 187:313–321

Li Q, Elimelech M (2004) Organic fouling and chemical cleaning of nanofiltration membranes: measurements and mechanisms. Environ Sci Technol 38:4683–4693

Mahlangu TO, Hoek E, Mamba BB, Verliefde A (2014) Influence of organic, colloidal and combined fouling on NF rejection of NaCl and carbamazepine: role of solute–foulant–membrane interactions and cake-enhanced concentration polarisation. J Membr Sci 471:35–46

Mahlangu TO et al (2016) Role of permeate flux and specific membrane-foulant-solute affinity interactions in transport of trace organic solutes through fouled nanofiltration (NF) membranes. J Membr Sci 518:203–215. https://doi.org/10.1016/j.memsci.2016.06.013

McCutcheon JR, Elimelech M (2006) Influence of concentrative and dilutive internal concentration polarization on flux behavior in forward osmosis. J Membr Sci 284:237–247

Miyabe K, Isogai R (2011) Estimation of molecular diffusivity in liquid phase systems by the Wilke–Chang equation. J Chromatogr A 1218:6639–6645

Mo Y, Xiao K, Shen Y, Huang X (2011) A new perspective on the effect of complexation between calcium and alginate on fouling during nanofiltration. Sep Purif Technol 82:121–127. https://doi.org/10.1016/j.seppur.2011.08.033

Mohammad AW, Teow YH, Ang WL, Chung YT, Oatley-Radcliffe DL, Hilal N (2015) Nanofiltration membranes review: recent advances

and future prospects. Desalination 356:226–254. https://doi.org/10.1016/j.desal.2014.10.043

Ng HY, Elimelech M (2004) Influence of colloidal fouling on rejection of trace organic contaminants by reverse osmosis. J Membr Sci 244:215–226

Nghiem LD, Hawkes S (2007) Effects of membrane fouling on the nanofiltration of pharmaceutically active compounds (PhACs): mechanisms and role of membrane pore size. Sep Purif Technol 57:176–184

Nyström M, Pihlajamäki A, Ehsani N (1994) Characterization of ultrafiltration membranes by simultaneous streaming potential and flux measurements. J Membr Sci 87:245–256

Plakas KV, Karabelas AJ (2012) Removal of pesticides from water by NF and RO membranes—a review. Desalination 287:255–265

Porter MC (1972) Concentration polarization with membrane ultrafiltration. Ind Eng Chem Prod Res Dev 11:234–248

Sadmani AHMA, Andrews RC, Bagley DM (2014) Nanofiltration of pharmaceutically active and endocrine disrupting compounds as a function of compound interactions with DOM fractions and cations in natural water. Sep Purif Technol 122:462–471. https://doi.org/10.1016/j.seppur.2013.12.003

Schäfer A, Mastrup M, Jensen RL (2002) Particle interactions and removal of trace contaminants from water and wastewaters

Schäfer A, Nghiem L, Waite T (2003) Removal of the natural hormone estrone from aqueous solutions using nanofiltration and reverse osmosis. Environ Sci Technol 37:182–188

Shan J, Hu J, Ong S (2009) Adsorption of neutral organic fractions in reclaimed water on RO/NF membrane. Sep Purif Technol 67:1–7

Snyder SA, Westerhoff P, Yoon Y, Sedlak DL (2003) Pharmaceuticals, personal care products, and endocrine disruptors in water: implications for the water industry. Environ Eng Sci 20:449–469

Verliefde AR et al (2009) Influence of membrane fouling by (pretreated) surface water on rejection of pharmaceutically active compounds (PhACs) by nanofiltration membranes. J Membr Sci 330:90–103

Vogel D, Simon A, Alturki AA, Bilitewski B, Price WE, Nghiem LD (2010) Effects of fouling and scaling on the retention of trace organic contaminants by a nanofiltration membrane: the role of cake-enhanced concentration polarisation. Sep Purif Technol 73:256–263. https://doi.org/10.1016/j.seppur.2010.04.010

Wang L-F, He D-Q, Chen W, Yu H-Q (2015a) Probing the roles of Ca^{2+} and Mg^{2+} in humic acids-induced ultrafiltration membrane fouling using an integrated approach. Water Res 81:325–332. https://doi.org/10.1016/j.watres.2015.06.009

Wang X-M, Li B, Zhang T, Li X-Y (2015b) Performance of nanofiltration membrane in rejecting trace organic compounds: experiment and model prediction. Desalination 370:7–16. https://doi.org/10.1016/j.desal.2015.05.010

Xu P, Drewes JE, Kim T-U, Bellona C, Amy G (2006) Effect of membrane fouling on transport of organic contaminants in NF/RO membrane applications. J Membr Sci 279:165–175

Yang L, Zhou J, She Q, Wan MP, Wang R, Chang VWC, Tang CY (2017) Role of calcium ions on the removal of haloacetic acids from swimming pool water by nanofiltration: mechanisms and implications. Water Res. https://doi.org/10.1016/j.watres.2016.11.040

Yangali-Quintanilla V, Sadmani A, McConville M, Kennedy M, Amy G (2009) Rejection of pharmaceutically active compounds and endocrine disrupting compounds by clean and fouled nanofiltration membranes. Water Res 43:2349–2362. https://doi.org/10.1016/j.watres.2009.02.027

Zhao C, Zhang J, He G, Wang T, Hou D, Luan Z (2013) Perfluorooctane sulfonate removal by nanofiltration membrane the role of calcium ions. Chem Eng J 233:224–232. https://doi.org/10.1016/j.cej.2013.08.027

Zhao C, Tang CY, Li P, Adrian P, Hu G (2016) Perfluorooctane sulfonate removal by nanofiltration membrane—the effect and interaction of magnesium ion/humic acid. J Membr Sci 503:31–41. https://doi.org/10.1016/j.memsci.2015.12.049